Materials Science and Engineering B78 (2000) 28–31

MATERIALS SCIENCE & ENGINEERING B

www.elsevier.com/locate/mseb

Photoluminescence properties of $Al_3GdB_4O_{12}$:Eu phosphors

W. Park [a,*], R.-Y. Lee [a,1], C.J. Summers [a], Y.R. Do [b], H.G Yang [b]

[a] *Phosphor Technology Center of Excellence, Manufacturing Research Center, Georgia Institute of Technology, Atlanta, GA 30332-0560, USA*

[b] *Material Technology Laboratory, Samsung SDI Co. Ltd., 575 Shin-Dong, Paldal-Gu, Suwon City, Kyungki-Do, South Korea 442-390*

Received 23 May 2000

Abstract

An investigation is reported of the photoluminescence (PL) properties of $Al_3GdB_4O_{12}$:Eu phosphors. Under vacuum ultraviolet excitation, $Al_3GdB_4O_{12}$:Eu exhibited a bright red luminescence with CIE chromaticity coordinates of (0.643, 0.356) with a PL intensity of 60% of the sodium salicylate standard. The PL spectrum showed a ground state splitting pattern consistent with D_3 symmetry. The PL excitation spectrum showed sharp lines due to the $^8S_{7/2}$–^6I_J and ^6P_J transitions of Gd^{3+} in addition to the f–f transitions of Eu^{3+}. The charge transfer band of Eu was observed at 250 nm and the host absorption band was detected at 157 nm. Time-resolved spectroscopy was performed to investigate the interaction between Gd and Eu ions. The energy transfer rate from Gd to Eu ions was found to be 17 000 s^{-1}. © 2000 Elsevier Science S.A. All rights reserved.

Keywords: Photoluminescence; Phosphors; Gd compound; Energy transfer

1. Introduction

The design of phosphors optimized for plasma display panels (PDP) involves a new set of considerations that was not included in the development of traditional lamp phosphors [1]. The excitation in a PDP is provided by the plasma of xenon and helium. The main emission of the plasma consists of 147 and 172 nm (8.4 and 7.2 eV) in comparison to the 254 nm (4.9 eV) line of mercury discharge used in fluorescent lamps [2]. The requirement that the phosphor host lattice absorb efficiently in the 147–180 nm range places new restrictions on the materials to be investigated. Thus, the issue of energy transfer from host to activator must be well understood. The energy transfer probability is generally proportional to the spectral overlap between the sensitizer and activator. Therefore, phosphors exhibiting a large energy mismatch between the host bandgap and the activator energy level are expected to show less efficient energy transfer, which will result in a smaller excitation efficiency. In this case, the presence of sensitizer ions, which provide intermediate energy levels through which the energy transfer from the host to activator occurs, will improve the efficiency. Another issue is maintenance. Since the phosphors are directly exposed to the plasma during the operation of the PDP, the host lattice must be rugged and resistant against ion bombardment and ultraviolet (UV) radiation. Therefore, the best candidate for new PDP phosphors must exhibit efficient energy transfer, high absorption in the UV, and good maintenance against UV radiation and ion bombardment.

The borates are exceptional materials because they are not refractory, but nonetheless exhibit excellent maintenance [3]. This is contradictory to the commonly accepted wisdom that high firing temperatures, as occur for the refractory materials, are essentially responsible for their good maintenance properties. The combination of good maintenance with low firing temperatures (typically lower than 1200°C) is additionally a great economic advantage. The borates also exhibit high absorption in the vacuum UV (VUV) region, especially when codoped with Gd. In this paper, we report the photoluminescence properties of $Al_3GdB_4O_{12}$:Eu in the VUV-visible region.

---

[*] Corresponding author. Tel.: +1-404-8940109; fax: +1-404-8945073.

E-mail address: won.park@gtri.gatech.edu (W. Park).

[1] Present address: Department of Materials Science and Engineering, Dankook University, Cheonan, Choongnam 330-714, Korea.

PII: S0921-5107(00)00509-2

2. Experiments

In this study, $Al_3GdB_4O_{12}$:Eu was synthesized by the solid state reaction technique. The starting materials, Al_2O_3, Gd_2O_3, Eu_2O_3 and H_3BO_3 were mixed stoichiometrically and ball milled for 4 h for uniform mixing. For photoluminescence (PL) measurements, a D_2 lamp was used for VUV–UV excitation and a Xe lamp was used for the UV-visible region. Pulsed excitation for the time-resolved spectroscopy was provided by an optical parametric oscillator (OPO) laser pumped by a Nd:YAG laser, which is tunable from 220 nm–1.8 μm and has a pulse width of 8 ns. The PL signal was detected by a thermoelectrically cooled GaAs photomultiplier tube (PMT) coupled with a 0.27 m monochromator. The PL measurement system was calibrated by using the standard tungsten lamp with factory-calibrated spectral irradiance output (Oriel 63358) and all the PL spectra reported in this paper were corrected for the system response.

In order to find the reaction temperature, thermal analysis was performed. Fig. 1 shows the differential thermal analysis (DTA)/thermal gravity (TG) curves. The TG curve shows a large drop between 100 and 200°C and the DTA-curve also shows two exothermic peaks in the same temperature region. This is due to the decomposition of boric acid, i.e. $2H_3BO_3 \rightarrow B_2O_3 + 3H_2O$. This decomposition is a two-stage process involving an intermediate HBO_2 phase, which can be seen clearly from the DTA curve. The DTA curve also exhibits an endothermic peak at 890°C, which corresponds to the formation of $Al_3GdB_4O_{12}$. Based on this result, a two-step heating process was adopted for the synthesis. The stoichiometric mixture of precursors was first heated to 500°C for 2 h and then to 1000°C for another 2 h. The first step was necessary to ensure the complete decomposition of boric acid. X-ray diffraction results showed that a significant portion of the phosphor was in the $GdBO_3$ phase along with some $Al_3GdB_4O_{12}$. In order to obtain single-phase material, 10% excess H_3BO_3 was added to the starting material mixture as a flux agent. The mixture was again ball milled for 4 h and fired using the two-step firing condition described above. After firing, the phosphor material was thoroughly washed to completely remove any residual flux material. The result of the X-ray analysis of the phosphor powders indicated that the major phase of the phosphor was $Al_3GdB_4O_{12}$ and the amount of $GdBO_3$ was very small.

3. Results and discussion

Under 147 nm excitation, $Al_3GdB_4O_{12}$:Eu was found to exhibit a strong red emission, characteristic of Eu^{3+} ions, with CIE chromaticity coordinates of (0.643, 0.356). This emission was comparable to that of the commercial $(Y,Gd)BO_3$:Eu phosphor. At the current stage of development, the best sample has a Eu concentration of 5 at.%, exhibiting a quantum efficiency of approximately 60% compared to the sodium salicylate standard. Further improvement will be possible by adjusting the firing temperature and by the addition of excess H_3BO_3 to suppress the formation of non-radiative defects. Fig. 2 shows the PL spectrum obtained for $Al_3GdB_4O_{12}$:Eu (5.0 at.%) under 274 nm

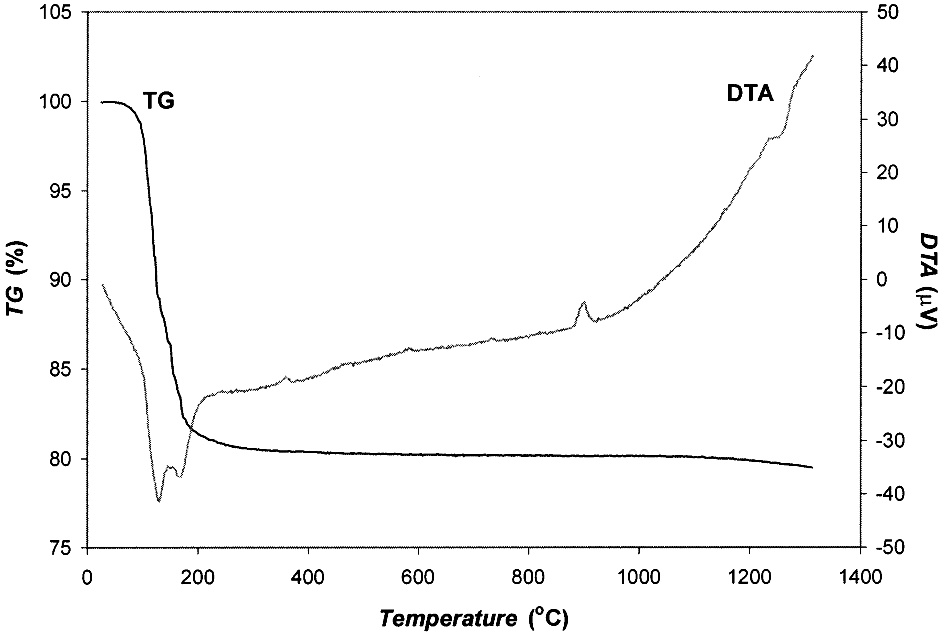

Fig. 1. TG/DTA analysis of $Al_3GdB_4O_{12}$ phosphor synthesis.

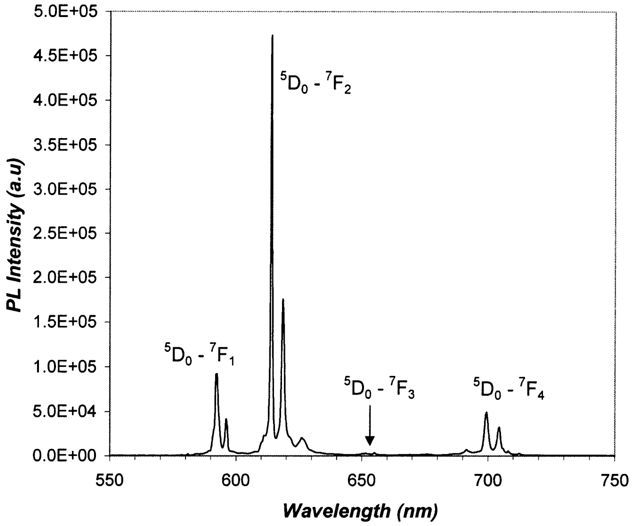

Fig. 2. PL spectrum of $Al_3GdB_4O_{12}$ phosphor under 274 nm UV excitation.

UV excitation. The spectrum is dominated by the line at 614 nm due to the $^5D_0$–$^7F_2$ transition of Eu^{3+}, which is typical of Eu^{3+} ions occupying sites with no inversion symmetry [4]. The spectrum also shows many additional lines due to the spin-orbit split ground states, ^7F_J ($J = 0$–6), each of which is further split by the crystal field. The two most intense emission lines, which are due to the $^5D_0$–$^7F_1$ and $^7F_2$ transitions, consist of two and three separate emission lines, respectively. $Al_3GdB_4O_{12}$ is known to crystallize in a hexagonal structure with the Eu sites possessing the D_3 symmetry[5]. Group theoretical considerations predict that for D_3 symmetry the crystal field should split the $^7F_1$ and $^7F_2$ levels into two and three Stark components, respectively. This is exactly what was observed experimentally, confirming the local site symmetry of the Eu ions and also indicating that there is no local distortion.

Fig. 3 shows the VUV–visible PLE spectrum for $Al_3GdB_4O_{12}$ with an Eu concentration of 5 at.%. In order to show the entire spectral range from VUV to visible, both the D_2 and Xe lamp excited PLE spectra are plotted together. The PLE spectra show features due to both Gd and Eu. The spectrum is dominated by an intense excitation peak at 394 nm due to the $^7F_0$–$^5L_6$ transition of the Eu^{3+} ion. Also observed are strong excitation lines due to the $^7F_0$–$^5D_1$ and $^5D_2$ transitions at 536 and 466 nm, respectively, in addition to many other sharp lines due to the various f–f transitions of Eu^{3+}. The sharp excitation lines at 274 and 311 nm are assigned to the $^8S_{7/2}$–^6I_J and ^6P_J transitions of Gd^{3+}, respectively [6]. This clearly shows that an efficient energy transfer occurs from Gd to Eu. The broad excitation band centered at 250 nm is assigned to a charge transfer transition between Eu and the neighboring oxygen anions. Finally, the broad excitation band at 157 nm is attributed to host absorption, because of its similar position to the host absorption of $Gd(BO_3)_3$ (159 nm) [7]. The excitation process is believed to be similar to that reported for $Gd(BO_3)_3$. That is, the host excitation is mediated by the excitation of the Gd sublattice, which allows efficient exciton migration through the lattice until a Eu activator ion is located to transfer energy and produce luminescence.

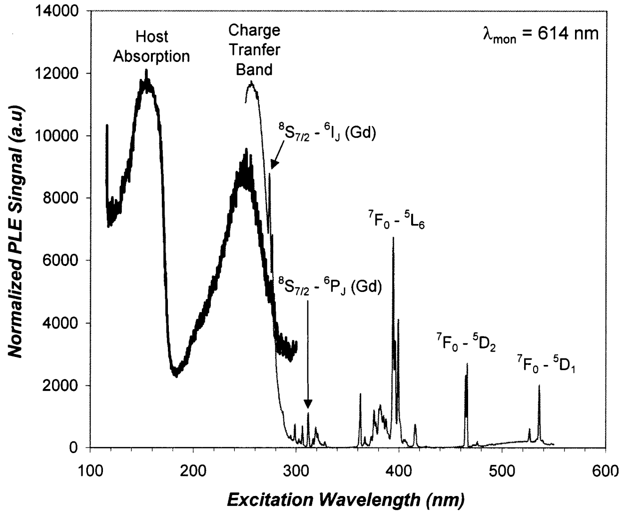

Fig. 3. PLE spectra in the VUV-visible region. D_2 lamp was used for 110–300 nm and Xe lamp was used for longer wavelengths.

To further investigate the interaction mechanism between the Gd and Eu ions, time-resolved spectroscopy was performed. Fig. 4 shows the luminescence decay of the Eu^{3+} emission at 10 K. When the charge transfer band of Eu was directly pumped by 250 nm excitation,

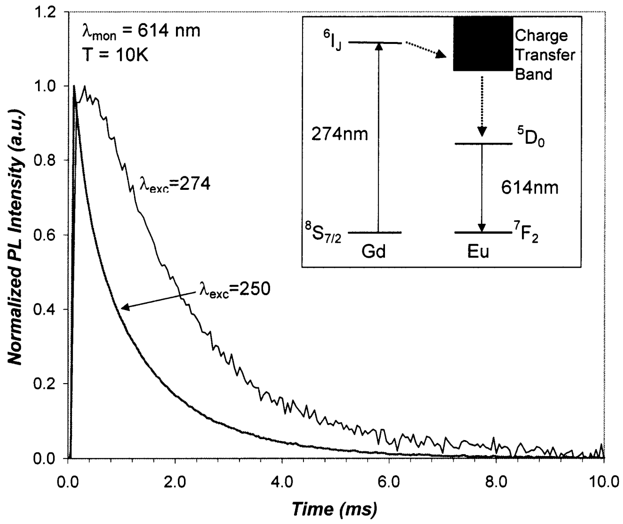

Fig. 4. 10 K luminescence decay curves for the 614 nm Eu^{3+} emission under 250 and 274 nm excitation. Inset: Schematic of the excitation process for the Eu ions through the energy transfer from Gd ions.

the luminescence showed a sharp rise followed by a nearly single exponential decay. The decay time was found to be 1.6 ms by numerically fitting the decay curve with an exponential function. When the excitation wavelength was changed to 274 nm, the position of the Gd^{3+} $^8S_{7/2}$–^6P_J transition, the Eu luminescence exhibited a delayed rise followed by a decay with approximately the same decay time as the 250 nm excitation. This slow rise was attributed to the finite transfer time involved in the Gd–Eu energy transfer process, as schematically shown in the inset of Fig. 4. The position of the maximum was shifted by approximately 200 μs compared to the charge transfer excitation at 250 nm. The rate equations governing the decay of Gd and Eu ions are

$$\frac{dN_G(t)}{dt} = -W_G N_G(t) - W_{ET} N_G(t),$$

$$\frac{dN_E(t)}{dt} = W_{ET} N_G(t) - W_E N_E(t),$$

where N_G and N_E are the density of excited Gd and Eu ions, W_G and W_E are the intrinsic decay rates of Gd and Eu, respectively, and W_{ET} is the energy transfer rate between Gd and Eu. If W_{ET} does not possess any time dependence, the general solution for $N_E(t)$ is

$$N_E(t) = W_{ET} e^{-W_E t} \int_0^t e^{W_E x} N_G(x)\, dx.$$

An analytical solution can be obtained if the Gd decay, $N_G(t)$, is assumed to be purely exponential

$$N_E(t) = \frac{N_G(0) W_{ET}}{W_G + W_{ET} - W_E}\left(e^{-W_E t} - e^{-(W_G + W_{ET})t}\right).$$

This result clearly predicts that the Eu luminescence should show a slow rise, reach a maximum, and then decay with either its own intrinsic lifetime or the Gd decay rate, whichever is the smaller. The condition for maximum emission intensity can be found by differentiating the above equation with respect to time, t, and setting it equal to zero, which gives

$$W_E e^{-W_E t_{max}} = (W_G + W_{ET}) e^{-(W_G + W_{ET}) t_{max}},$$

where t_{max} is the time for the Eu luminescence to reach a maximum.

From the experimental results shown in Fig. 4, we obtain $W_E = 630\ s^{-1}$ and $t_{max} = 200$ μs. Then, from the above equation, we found that $W_G + W_{ET} = 17\ 000\ s^{-1}$. Considering that the Gd^{3+} luminescence usually exhibits decay times on the order of a few milliseconds, due to the forbidden nature of f–f transition, it is expected that $W_G \sim 400\ s^{-1}$ and thus $W \ll W_{ET}$. Therefore, the energy transfer rate from Gd to Eu in $Al_3GdB_4O_{12}$:Eu was estimated to be approximately 17 000 s^{-1}, which corresponds to an energy transfer time of 60 μs. This value of W_{ET} was smaller than that observed for $GdAlO_3$:Eu, which was on the order of $10^6\ s^{-1}$ [8]. This difference is attributed to the larger interionic distance in $Al_3GdB_4O_{12}$:Eu, where a BO^{-3} group separates each nearest neighbor Gd ions, yielding a relatively large nearest Gd–Gd distance of 5.9 Å. On the other hand, the distance between Gd–Eu pairs is only 3.8 Å in $GdAlO_3$:Eu [9]. The large interionic distance in $Al_3GdB_4O_{12}$:Eu naturally leads to a lower energy transfer rate, because the energy transfer rate is a strongly decaying function of interionic distance [10].

4. Conclusions

In summary, we report the photoluminescence properties of $Al_3GdB_4O_{12}$:Eu under VUV and UV excitation. A synthesis route involving two-step firing was used to obtain single-phase material. Under 147 nm VUV excitation, $Al_3GdB_4O_{12}$:Eu showed good quantum efficiency, approximately 60% of the sodium salicylate standard. It is expected that further improvement would be possible by refining the synthesis process. The PL spectrum was consistent with the D_3 symmetry for Eu sites, indicating that there was no local distortion. PLE measurements showed that an efficient energy transfer occurs between Gd and Eu ions. The charge transfer band of Eu and the host absorption band were also observed at 250 and 157 nm, respectively. The energy transfer rate between Gd and Eu ions was found to be 17 000 s^{-1}.

References

[1] C.R. Ronda, J. Lumin. 72–74 (1997) 49.

[2] T. Kamegaya, H. Matsuzaki, M. Yokozawa, IEEE Trans. Electron Devices ED–25 (1978) 1094.

[3] R.G. Pappalardo, in: B. Di Bartolo, G. Armagan (Eds.), Spectroscopy of Solid-State Laser-Type Materials, Plenum Press, New York, 1987, p. 397.

[4] G. Blasse, Chem. Phys. Lett. 20 (1973) 573.

[5] A.A. Ballman, Am. Mineral. 47 (1962) 1380.

[6] R.T. Wegh, H. Donker, A. Meijerink, R.J. Lamminmaki, J. Holsa, Phys. Rev. B 56 (1997) 13841.

[7] E. Antic-Fidancev, J.C. Krupa, M. Lemaiter-Blaise, Mater. Sci. Forum 315–317 (1999) 373.

[8] G. Blasse, Prog. Solid State Chem. 18 (1988) 79.

[9] A.J. De Vries, W.J.J. Smeets, G. Blasse, Mat. Chem. Phys. 18 (1987) 81.

[10] W. Park, T.C. Jones, W. Tong, S. Schön, M. Chaichimansour, B.K. Wagner, C.J. Summers, J. Appl. Phys. 84 (1998) 6852.